ARVC-Related Mutations in Divergent Region 3 Alter Functional Properties of the Cardiac Ryanodine Receptor

Andrea Koop,* Petra Goldmann,* S. R. Wayne Chen,† Rolf Thieleczek,* and Magdolna Varsányi*
*Institut für Physiologische Chemie, Abteilung Biochemie Supramolekularer Systeme, Ruhr-Universität Bochum, 44780 Bochum, Germany; and †Departments of Physiology and Biophysics and of Biochemistry and Molecular Biology, University of Calgary, Calgary, Alberta T2N 4N1, Canada

ABSTRACT Two single-nucleotide polymorphisms in the type 2 ryanodine receptor (RyR2) leading to the nonsynonymous amino acid replacements G1885E and G1886S are associated with arrhythmogenic right ventricular cardiomyopathy in patients who are carrying both of the corresponding RyR2 alleles. The functional properties of HEK293 cell lines isogenically expressing RyR2 mutants associated with arrhythmogenic right ventricular cardiomyopathy, RyR2-G1885E, RyR2-G1886S, RyR2-G1886D (mimicking a constitutively phosphorylated Ser^{1886}), and the double mutant RyR2-G1885E/G1886S were investigated by analyzing the intracellular Ca^{2+} release activity resulting from store-overload-induced calcium release. The substitution of serine for Gly^{1886} caused a significant increase in the cellular Ca^{2+} oscillation activity compared with RyR2 wild-type-expressing HEK293 cells. It was even more pronounced if glycine 1885 or 1886 was replaced by the acidic amino acids glutamate (G1885E) or aspartate (G1886D). Surprisingly, when both substitutions were introduced in the same RyR2 subunit (RyR2-G1885E/G1886S), the store-overload-induced calcium release activity was nearly completely abolished, although the Ca^{2+} loading of the intracellular stores was markedly enhanced, and the channel still displayed substantial Ca^{2+} release on stimulation by 5 mM caffeine. These results suggest that the adjacent glycines 1885 and 1886, located in the divergent region 3, are critical for the function and regulation of RyR2.

INTRODUCTION

The cardiac ryanodine receptor (RyR2) located in the sarcoplasmic reticulum (SR) membrane functions as a Ca^{2+} release channel through which, on Ca^{2+}-induced Ca^{2+} release, Ca^{2+} flows from the lumen of the SR into the cytoplasm and activates cardiomyocyte contraction. It thus plays a crucial role in cardiac excitation-contraction coupling (for review see Fill and Copello (1)). The large cytoplasmic domain of the functional tetrameric RyR2 channel possesses the Ca^{2+} binding sites for initiation of Ca^{2+}-induced Ca^{2+} release as well as binding sites for channel modulators such as FKBP12.6, calmodulin, and ATP and target sites for phosphorylation by different protein kinases such as PKA, PKC, PKG, and CaMKII (2,3). Three domains have been coarsely defined in RyR2, the N-terminal, the central, and the C-terminal domains, where mutations leading to cardiomyopathies including arrhythmogenic right ventricular cardiomyopathy (ARVC) and catecholaminergic polymorphic ventricular tachycardia have been located (4). Disease-causing mutations in the N-terminal and central domains have been localized to the clamp-shaped structure of RyR2 (5–7), and these mutations alter the sensitivity of channel activation by luminal Ca^{2+} (8,9). Interaction of these two domains stabilizes the closed state of the Ca^{2+} release channel, and mutations in this region might weaken this interdomain interaction, leading to a decline of tight channel control, lowering of the barrier for Ca^{2+} release, and an increase in Ca^{2+} leakage from the SR (10). Dysfunctional RyR2 has been implicated in the generation of cardiomyopathies (for a review see Thomas et al. (11)), and diastolic Ca^{2+} release by a leaky cardiac Ca^{2+} release channel is thought to be responsible for the development of arrhythmogenesis (12).

Recently, we have identified two single-nucleotide polymorphisms (SNPs) in adjacent codons of the RYR2 gene in patients suffering from ARVC that lead to the nonsynonymous amino acid exchanges G1885E and G1886S in a composite heterozygous fashion (13). The location affected by the mutations is part of the cardiac-specific divergent region 3 (DR3 domain) of RyR2, which is believed to be involved in regulation of the Ca^{2+} release channel (6). The combination of these two polymorphisms is associated with ARVC in a subgroup of patients. RyR2 isolated from the explanted heart of such an ARVC patient shows altered channel characteristics and markedly enhanced open probability at diastolic Ca^{2+} concentration. Because of the heterozygous combination of the SNPs, the actual subunit composition of this leaky RyR2 channel is not known. The functional channel can be either a homotetramer encoded by either of the two alleles or a heterotetramer because of mixed expression of both alleles. Expression of G1886S would create

Submitted September 20, 2007, and accepted for publication January 30, 2008.

Address reprint requests to Magdolna Varsányi, Institut für Physiologische Chemie, Abteilung Biochemie Supramolekularer Systeme, Ruhr-Universität Bochum, 44780 Bochum, Germany. Tel.: +49-234-3225291; Fax: 49-234-3214193; E-mail: magdolna.varsanyi@ruhr-uni-bochum.de.

Editor: David A. Eisner.

0006-3495/08/06/4668/10 $2.00

doi: 10.1529/biophysj.107.122382

a putative PKC phosphorylation site in RyR2, which might confer PKC-mediated modulation of the Ca^{2+} release channel.

In this work, we investigated functional properties of defined RyR2 mutants related to the ARVC-associated alterations G1885E and G1886S: RyR2-G1885E, RyR2-G1886S, RyR2-G1886D mimicking a putatively phosphorylated Ser^{1886}, and RyR2-G1885E/G1886S with both nonsynonymous amino acid exchanges in the same RyR2 subunit. The identified SNPs were introduced into mouse RYR2 cDNA, which then was used to generate stable, inducible HEK293 cell lines, each expressing a defined isogenic RyR2. The store-overload-induced calcium release (SOICR) activity of these cell lines was investigated quantitatively by single-cell Ca^{2+} imaging and compared with the Ca^{2+} release behavior of RyR2 wild-type (RyR2-WT)-expressing HEK293 cells. RyR2 protein purified from these cell lines was characterized biochemically, and the phosphorylation of RyR2-G1886S was studied using the protein kinases PKA, PKG, PKC, and CaMKII. The replacement of a glycine at the positions 1885 and 1886 of human RyR2 by an acidic residue (G1885E, G1886D) substantially enhanced the activity of the homotetrameric Ca^{2+} release channel. This is true, albeit to a lesser extent, also for G1886S, which is not a target of any of the protein kinases investigated. Surprisingly, the double mutant, G1885E/G1886S, was nearly completely inactive. This indicates that these two positions in the RyR2 primary sequence mark a sensitive spot in the DR3 domain that is involved in the control of the Ca^{2+} release properties of the channel.

EXPERIMENTAL PROCEDURES

Materials

Monoclonal RyR2 antibody (34c) was obtained from Acris Antibodies (Hiddenhausen, Germany) FITC-labeled antimouse secondary antibody and polyclonal anti-FKBP antibody were from Alexis (Lausen, Switzerland), and peroxidase coupled antimouse and antirabbit secondary antibodies were from MBI Fermentas (Madison, WI). Soybean phosphatidylcholine was purchased from Avanti Polar Lipids (Alabaster, AL), CHAPS and other reagents were from Sigma (St. Louis, MO). Activated EAH Sepharose, *N*-ethyl-*N′*(3-dimethylamino-propyl) carbodiimid (EDC), ECL kit and hyperfilm were obtained from Amersham (Little Chalfont, Bucks, UK). Talon affinity matrix was from Clontech (Mountainview, CA) and Restore Western Blot Stripping Buffer from Pierce (Rockford, IL). Ca^{2+} fluorescence indicators fura-2 AM and fluo-3 AM as well as hygromycin and tetracycline were purchased from Invitrogen (Carlsbad, CA).

Site-directed mutagenesis and DNA transfection

To generate the RyR2 mutants G1885E, G1886S, G1886D, and the double mutant G1885E/G1886S, the corresponding SNPs were introduced into the full-length mouse RyR2 cDNA using the overlap extension PCR method as described by Ho et al. (14). It is of note that the sequence of the human codons affected by the SNPs, 5653–5658, is homologous to the mouse RyR2 cDNA codon sequence 5650-5655; however, in this article, instead of the changed nucleotide sequence, the resulting amino acid exchange corresponding to the human sequence is used. The sequences of the primers used for mutagenesis were as follows: RyR2-G1885E sense, 5′-GCCAAAGAGGGTAAAAGGCCC-3′, and antisense, 5′-TTTACCCTCTTTGGCTTCTTCT T-3′; RyR2-G1886S sense, 5′-AAAGGGAGTAAAAGGCCCAAG-3′, and antisense, 5′-CCTTT TACTCCCTTTGGCTTC-3′; RyR2-G1886D sense, 5′-AAAGGGGATAAAAGGCCCAAG-3′, and antisense, 5′-CCTTTTATCCCCTTTGGCTTC-3′; RyR2-G1885E/G1886S sense, 5′-GCC AAAGAGAGTAAAAGGCCCAAG-3′, and antisense, 5′-CCTTTTACTCTCTTTGGCTTCTT C-3′. The sequences of the flanking (outer) primers were, sense, 5′-AGTGAACGCCAAGGCTG G-3′, and antisense, 5′-AACGTACTGAAGTAATATGGACTT-3′. The RyR2 cDNA fragments containing the mutations were cloned back into the original position of the RyR2 cDNA sequence to replace the wild-type sequence. After confirmation of the mutations by DNA sequencing, the mutated RyR2 cDNAs were used for transfection of HEK293 cells using the Ca^{2+} phosphate precipitation method as described in detail by Li and Chen (15).

Generation of stable, inducible HEK293 cell lines

Flp-In TRex-293 cells (Invitrogen) were cotransfected with the inducible expression vector pcDNA5/FRT/TO containing RyR2 wild-type or RyR2 mutant cDNA and the pOG44 vector encoding the Flp-recombinase as described by Jiang et al. (8). Each HEK293 cell line was tested for RyR2 expression using Western blotting, immunocytofluorescent staining, and [^{3}H]ryanodine binding.

Single-cell Ca^{2+} imaging

Intracellular Ca^{2+} transients in HEK293 cells expressing wild-type and mutant RyR2, respectively, were measured using single-cell Ca^{2+} imaging as described previously (8). Briefly, cells grown on glass coverslips for 20–24 h after induction by 1 μg/ml tetracycline were loaded with the fluorescent Ca^{2+} indicator dye fura-2 acetoxymethyl ester (fura-2 AM, 5 μM) in Krebs-Ringer-Hepes (KRH) buffer (125 mM NaCl, 5 mM KCl, 1.2 mM KH_2PO_4, 6 mM glucose, 1.2 mM $MgCl_2$, 25 mM Hepes, pH 7.4) plus 0.02% pluronic F-127 (Molecular Probes, Eugene, OR) and 0.1 mg/ml BSA for 20 min at room temperature. The coverslips were mounted in a perfusion chamber (Warner Instruments, Hamden, CT) on a Zeiss (Jena, Germany) Axiovert 135 microscope and continuously perfused at room temperature with KRH buffer containing increasing concentrations of $CaCl_2$ ($[Ca^{2+}]_o$ = 0, 0.1, 0.2, 0.3, 0.5, and 1.0 mM). Each of these perfusion intervals lasted for 5 min. Fura-2 fluorescence was recorded at a sampling frequency of 0.25 Hz using a Fluor ×20 objective and a Chroma filter set with the ImageMaster System and a DeltaRAM rapid wavelength-switching illuminator (Photon Technology International, Lawrenceville, NJ). The stored Ca^{2+} of HEK293 cells expressing the various RyR2 was assessed after the final perfusion with 1 mM Ca^{2+} by a challenge with 5 mM caffeine in KRH containing 1 mM Ca^{2+}. The recorded fura-2 fluorescence traces were analyzed using a computer program written in MATLAB. Only those traces that contain at least one fluorescence value greater than two times the median fluorescence value during the perfusion with Ca^{2+}-free KRH were considered for analysis of intracellular Ca^{2+} release. This excludes those stably RyR2-transfected HEK293 cells that do not respond to caffeine with a substantial Ca^{2+} release from their internal stores. Furthermore, cells showing fluorescence traces with minimal (one time point) or prolonged threshold crossings (>5 time points) were individually inspected and rejected from further analysis in case of untypical Ca^{2+} transients. Traces with large amplitudes (fura-2 ratios of 6–8) were inspected and treated as indicated. Traces with larger ratios (>8) were eliminated. The relation between Ca^{2+} oscillation frequency and $[Ca^{2+}]_o$ of individual cells was determined from the number of threshold crossings within the time interval corresponding to a given $[Ca^{2+}]_o$.

Analysis of the $[Ca^{2+}]_o$-dependent Ca^{2+} oscillation behavior of RyR2-expressing HEK293 cells

The Ca^{2+} oscillation frequency of different RyR2-expressing HEK293 cell lines changes with the extracellular Ca^{2+} concentration $[Ca^{2+}]_o$. If, for a

specific RyR2-expressing HEK293 cell line, $N(f)$ denotes the number of cells oscillating with a certain frequency f, and N is the total number of oscillating cells, the relative number of cells obeying certain discrete Ca^{2+} oscillation frequencies $f = 0, 0.2, 0.4, \ldots, f_{max}$ (min^{-1})—determined by the number of Ca^{2+} transients during a 5-min $[Ca^{2+}]_o$ interval—is given by $p(f) = N(f)/N$. With increasing $[Ca^{2+}]_o$, the bandwidth i of the observed discrete frequencies $f_1, \ldots, f_i$ increases. For all $[Ca^{2+}]_o$, the relative number of oscillating cells, cumulatively summed up over the whole observed frequency bandwidth, will approach 1 with increasing oscillation frequency. This cumulative relative oscillation frequency distribution (CROFD) is given by

$$q(f) = \sum_i (p(f_i)), \text{ with } f_1 = 0\,\text{min}^{-1} \text{ and } \lim_{f \to f_{max}} (q(f)) = 1. \quad (1)$$

For all $[Ca^{2+}]_o$ used, the CROFD obtained can well be described by the empirical function

$$q(f) = q_0 + (1 - q_0) \times (g \times f)^n / (1 + (g \times f)^n) \quad (2)$$

with $q = q_0$ for $f = 0$ and $q = 1$ for $f \gg 1/g$. The characteristic parameters q_0, g, and n were obtained from fits to the CROFD measured at $[Ca^{2+}]_o$ of 0 to 1 mM. According to the experimental results obtained, g and q_0 are $[Ca^{2+}]_o$-dependent parameters that can be approximated by the functions

$$g([Ca^{2+}]_0) = g_0 - h \times [Ca^{2+}]_0 \quad (3)$$

$$q_0([Ca^{2+}]_0) = 1 - ([Ca^{2+}]_0/K_S)^m / (1 + ([Ca^{2+}]_0/K_S)^m), \quad (4)$$

the parameters of which were determined by fits to the measured data. The relative number of cells oscillating at a given $[Ca^{2+}]_o$ with a frequency bandwidth $f_1, \ldots, f_i$ can be obtained from the CROFD by

$$p(f_j, [Ca^{2+}]_0) = q(f_j, [Ca^{2+}]_0) - q(f_{j-1}, [Ca^{2+}]_0), j = 2, \ldots, i \quad (5)$$

and $p(f_1, [Ca^{2+}]_0) = q(f_1, [Ca^{2+}]_0)$. Equations 2 and 5 together with the obtained fit parameters describe relative oscillation frequency distributions up to a limiting $[Ca^{2+}]_0^{lim} = g_0/h$. The image recording frequency used of 15 frames/min was three times the maximum observed Ca^{2+} oscillation frequency (~5 min^{-1}) and thus sufficient to exclude limitations by the recording process.

Generation and purification of phosphorylation state- and site-specific anti-RyR2 antibodies

The individually designed polyclonal antisera and the synthetic peptides corresponding to the sequences of the mouse RyR2 were obtained from NeoMPS (Strasbourg, France). The following phosphopeptides and nonphosphopeptides were constructed: H^+-GGAKGS(PO_3)KRPK-AHX-Y-OH (pSer-1886) and H^+-GGAKGSKRPK-AHX-Y-OH (Ser-1886). These are unique among the known phosphopeptide sequences, and they are typical for RyR2 according to a BLASTP2.2.5 database search. To generate antibodies to the two peptides, two rabbits each were immunized with the above peptides covalently coupled to ovalbumin. IgG fractions were obtained after ammonium sulfate precipitation according to Javois (16) and subjected to affinity chromatography over carbodiimid-activated EAH Sepharose 4B (Amersham Biosciences) coupled with phosphopeptides and nonphosphopeptides according to manufacturer's instructions. The columns were reused several times and stored in water at 4°C. To obtain the phosphospecific antibodies and to eliminate the nonphospho- and nonspecific antibodies, the IgG fraction was first applied to the nonphosphopeptide affinity column. The breakthrough containing phosphopeptide antibodies obtained by washing the column with BBS buffer was applied to the phosphopeptide affinity column. Phosphopeptide antibodies were eluted with 0.1 M glycine, 0.5 M NaCl, pH 2.7, into tubes containing NaOH to neutralize the pH. Nonphosphopeptide antibodies were purified analogously by first applying the IgG fraction to a column prebound with the phosphopeptide. The resulting flowthrough was then applied to the nonphosphopeptide affinity column. Immunoreactivity and -specificity of the affinity-purified phospho- and nonphosphopeptide antibodies were determined by means of ELISA. Preimmune sera showed no immunoreactivity.

Human recombinant FKBP12.6

The plasmid construct for the expression of the N-terminal polyhistidine-tagged FKBP12.6 fusion protein was generated using the TOPO-TA cloning kit (Invitrogen). As template for amplification, a human brain total cDNA (Clontech) was used with the following primers: sense, 5′-ATGGGCGTG-GAGATCGAGACCATC-3′, and antisense, 5′-TCACTCTAAGTTGAG-CAG CTCCACGTC-3′. After amplification, the PCR product was ligated into the expression vector pCRT7/NT TOPO (Invitrogen), and the sequence of the cloned construct was confirmed by DNA sequencing. After transformation of chemical competent BL21(DE3) *E. coli*, protein overexpression was induced by 0.4 mM isopropyl-β-thiogalactopyranoside. The recombinant polyhistidine-tagged FKBP12.6 fusion protein was obtained from the supernatant of the cell homogenate by means of affinity chromatography columns (Protino Ni-Ted kit, Macherey-Nagel, Düren, Germany).

Preparation of cell lysate, solubilization, and enrichment of the expressed RyR2 and ryanodine binding assay

Cell lysates were obtained from stable, inducible HEK293 cells grown for various durations after induction by 1 μg/ml tetracycline as described in detail by Kong et al. (17). Recombinant RyR2 proteins were further enriched either by sucrose density gradient centrifugation (7–25% w/v) for 16 h at 100,000 × *g* (13) or by affinity chromatography using Talon Affinity matrix (Clontech) prebound with purified 300 μg His-tagged FKBP12.6 fusion protein for 18 h at 4°C. After sedimentation and washing with PBS buffer, the sediment containing the RyR2-FKBP12.6 complex-bound beads was used directly as substrate in phosphorylation assays. The binding of RyR2 to the FKBP12.6-loaded matrix was confirmed by SDS-PAGE and Western blotting after elution of the RyR2-FKBP12.6 complex from the beads by SDS sample buffer. [^{3}H]Ryanodine binding assays were carried out with different RyR2 variants as described by Jiang et al. (9).

Phosphorylation of Ser^{1886} in RyR2-G1886S by various protein kinases

Recombinant RyR2 obtained in different ways was used as a substrate for protein kinases previously activity-optimized with model peptides and proteins, respectively, according to the instructions provided by the suppliers. PKA catalytic subunit was a generous gift from Dr. Friedrich Herberg, Universität Kassel, Germany. Recombinant PKG was purchased from Alexis (Lausen, Switzerland), catalytic subunit of native PKC of rat brain was obtained from Calbiochem (La Jolla, CA), and recombinant CaMKII was from New England Biolabs (Ipswich, MA). RyR2 in the following states of purity were used: RyR2 in cell lysate, enriched by sucrose gradient centrifugation, or purified by affinity chromatography over FKBP12.6-bound Talon Sepharose beads. Phosphorylation by catalytic subunit of PKA was carried out in a buffer containing 10 mM MOPS, pH 7.0, 200 mM KCl, 1.5 mM DTT, 0.5 mM [γ-^{32}P]ATP, and 50 nM ocadaic acid.

Statistical evaluation

Mean values are presented as mean ± SE, and statistical comparison of data corresponding to the different RyR2 was carried out using one-way ANOVA

with Tukey's posttest. An error probability $p < 0.05$ was considered significant and is indicated where applicable.

RESULTS

Construction and generation of stable, inducible HEK293 cell lines expressing RyR2-WT, RyR2-G1885E, RyR2-G1886S, RyR2-G1886D, and RyR2-G1885E/G1886S

We have previously shown that a composite heterozygous SNP combination leading to the nonsynonymous exchanges G1885E and G1886S in the human RyR2 1), is associated with ARVC, 2), leads to a substantially increased diastolic open probability of RyR2 from a terminally failing heart of such a patient, and 3), may contain a PKC phosphorylation site created by one of the mutations, G1886S (13). The actual tetrameric subunit combination(s) of the functional RyR2 in human hearts of this RyR2 genotype is not known. Two possible compositions resulting from homozygous combinations are given by RyR2-G1885E and RyR2-G1886S, respectively, which were recombinantly generated. The latter represents the homotetramer with the suggested putative PKC phosphorylation site.

Stable, inducible HEK293 cell lines expressing the ARVC-related RyR2 mutants G1885E and G1886S were generated according to the method of Jiang et al. (8). Additionally, a cell line that stably expresses RyR2-G1886D, mimicking a constitutively phosphorylated Ser^{1886}, and a further one with both mutations in a single RyR2 subunit (RyR2-G1885E/G1886S) were established. The functional properties of these RyR2 variants were studied by measuring the SOICR activity of the RyR2-expressing HEK293 cells and by phosphorylation assays using purified RyR2-G1886S as a substrate for the protein kinases PKC, PKA, PKG, and CaMKII.

The expression of the variant RyR2 proteins in HEK293 cell lines was confirmed by immunofluorescent staining (Fig. 1, *A–F*) and Western blotting (Fig. 1 *G*) using monoclonal RyR2 antibody. This antibody detected a high-molecular-weight band in the HEK293 cell lines expressing RyR2 (Fig. 1, *B–G*) but not in the parental cells transfected with the control vector DNA (Fig. 1 *A*).

Biochemical characterization of the different RyR2 mutants

To determine whether the expressed RyR2-WT, RyR2-G1885E, RyR2-G1886S, RyR2-G1886D, and RyR2-G1885E/G1886S, respectively, function as Ca^{2+} release channels, we measured intracellular Ca^{2+} release in HEK293 cells expressing the various RyR2 forms using the fluorescent Ca^{2+} indicator dye fluo-3 acetoxymethyl ester. As shown in Fig. 2 *A*, all RyR2-expressing HEK293 cell lines displayed comparable Ca^{2+} transients in response to repeated stimulation by caffeine, a well-known activator of RyR2. The normalized caffeine dose-response curves obtained from the traces shown in Fig. 2 *A* were similar for RyR2-WT, RyR2-G1885E, RyR2-G1886S, and RyR2-G1886D, with half-maximum responses in the range of 0.11–0.20 mM caffeine (Fig. 2 *B*). For RyR2-G1885E/G1886S the half-maximum response was observed at 0.40 mM caffeine. Because the caffeine activation procedure was the same for all cell lines, these data suggest that the doubly mutated RyR2 is relatively less sensitive to caffeine than the other RyR2 variants ($p < 0.001$). The Ca^{2+}-dependent [^{3}H]ryanodine binding to the different RyR2 (Fig. 2 *D*) reaches half-saturation at about the same Ca^{2+} concentration but rises with a markedly reduced Ca^{2+} cooperativity in case of RyR2-G1885E/G1886S compared with the other RyR2 variants ($p < 0.001$). On the other hand, the well-known suppression (18) of the caffeine-induced Ca^{2+} release by ryanodine (Fig. 2 *C*, *b* and *c*) after it has gained access to the open state of the channel induced by

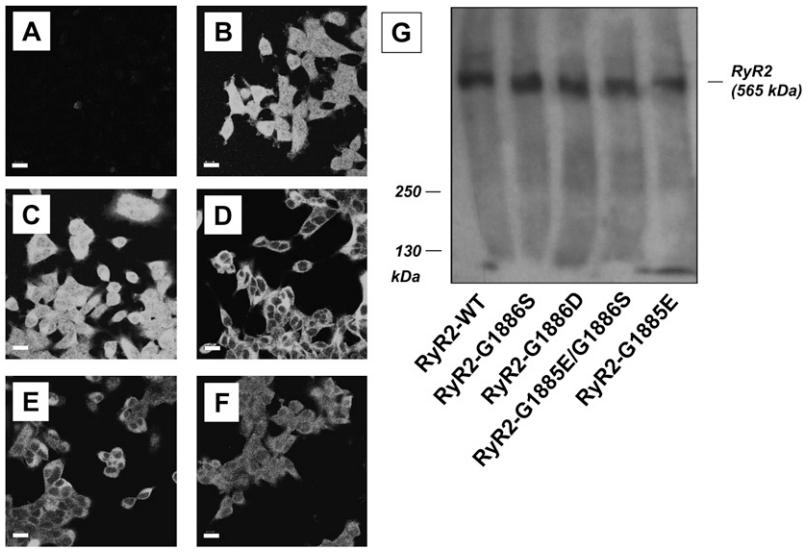

FIGURE 1 Immunofluorescent staining (*A–F*) and Western blot analysis (*G*) of stable, inducible HEK293 cell lines expressing RyR2-WT (*B*), RyR2-G1886S (*C*), RyR2-G1886D (*D*), RyR2-G1885E (*E*), and RyR2-G1885E/G1886S (*F*), respectively. (*A–F*) Stable, inducible HEK293 cells expressing the different RyR2 (*B–F*) as well as parental HEK293 cells transfected with empty expression vector pcDNA5/FRT/TO (*A*) were fixed and permeabilized 24 h after induction by tetracycline. RyR2 proteins were detected using monoclonal RyR2 antibody and secondary FITC-conjugated antimouse IgG antibody (scale bar, 20 μm). (*G*) Cell lysates were prepared from the HEK293 cell lines shown in *B* to *F*. RyR2 proteins were separated by SDS-PAGE and immunoblotted with RyR2 antibody and secondary HRP-coupled antimouse IgG antibody.

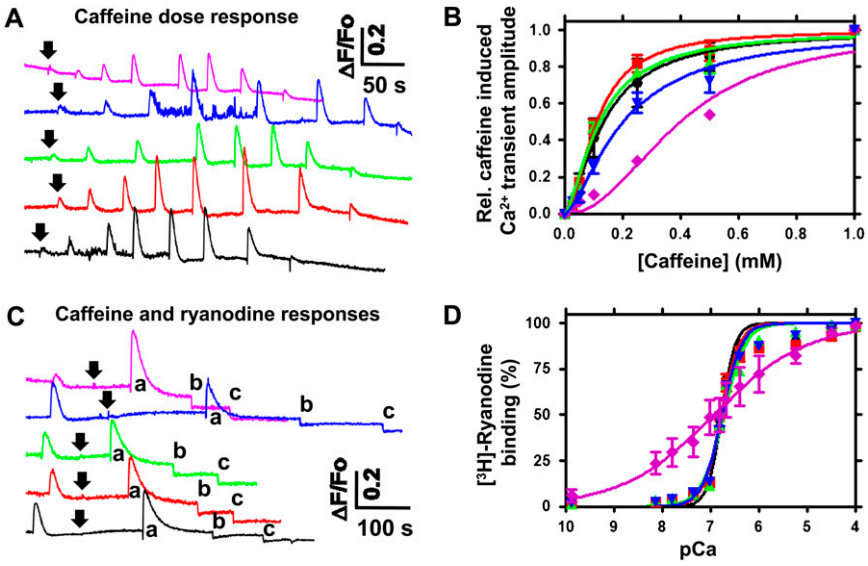

FIGURE 2 Fluo-3 fluorescence of HEK293 cells (*A–C*) expressing RyR2-WT, RyR2-G1886S, RyR2-G1886D, RyR2-G1885E, and RyR2-G1885E/G1886S, respectively, in response to caffeine (*A, B, C*) and ryanodine (*C*) and Ca^{2+}-dependent ryanodine binding to the different RyR2 mutants (*D*). The traces and curves shown are color coded: RyR2-WT (*black*); RyR2-G1886S (*red*); RyR2-G1886D (*green*); RyR2-G1885E (*blue*); RyR2-G1885E/G1886S (*magenta*). (*A*) Fluorescence signals of cells expressing a specific RyR2 variant in response to successive additions of caffeine (mM): 0.025, 0.05, 0.1, 0.25, 0.5, 1, 2.5, and 5. The first addition is marked by an arrow, and the following ones can be identified by the induced Ca^{2+} transients. (*B*) Caffeine-induced Ca^{2+} transient amplitude as function of the applied caffeine concentration normalized to the maximum response obtained at 1 mM caffeine. The datasets ($n = 4$) are approximated by a sigmoidal function of the type $y = x^h/(K_D{}^h + x^h)$. (*C*) Blockage of the expressed RyR2 variants by 100 μM ryanodine. After an initial stimulation with 0.25 mM caffeine (*first peak*) followed by the ryanodine addition (*arrow*), the cells are challenged by three successive additions of 2.5 mM caffeine (*a*, *b*, and *c*). (*D*) Ca^{2+}-dependent ryanodine binding to the RyR2 variants. Lysates (30 μl) prepared from the RyR2-expressing cell lines were incubated with 5 nM [^{3}H]ryanodine. The datasets are approximated by the sigmoidal function given above. The Ca^{2+} concentrations at half-maximum ryanodine binding, K_D, and Hill coefficients, h, are 165 ± 3 nM and 3.08 ± 0.21 ($n = 6$) for RyR2-WT, 163 ± 6 nM and 2.36 ± 0.23 ($n = 6$) for RyR2-G1886S, 179 ± 6 nM and 1.93 ± 0.13 ($n = 6$) for RyR2-G1886D, 168 ± 5 nM and 2.16 ± 0.15 ($n = 6$) for RyR2-G1885E, and 117 ± 27 nM and 0.45 ± 0.06 ($n = 5$) for RyR2-G1885E/G1886S.

caffeine (Fig. 2 *C*, *a*) is well preserved for all the expressed RyR2 variants. These data indicate comparable, wild-type-like channel function for the mutants RyR2-G1885E, RyR2-G1886S, and RyR2-G1886D and altered channel properties for the double mutant RyR2-G1885E/G1886S.

Phosphorylation of Ser^{1886} in RyR2-G1886S

The phosphorylation of Ser^{1886}, which is a putative PKC phosphorylation site in the RyR2 mutant G1886S (13), was investigated using recombinant RyR2-G1886S protein of different purification states as a substrate for PKC and other protein kinases, PKA, PKG, and CaMKII, known to phosphorylate RyR2 (for review see Meissner (3) and Xiao et al. (19)). The substrate was presented in three different purification grades: RyR2-G1886S in crude cell lysate (Fig. 3 *A*), RyR2-G1886S bound to FKBP12.6-coupled Sepharose beads (Fig. 3 *B*), and RyR2-G1886S highly enriched by sucrose density centrifugation (Fig. 3 *C*). All tested kinases phosphorylate the mutant channel protein (row 4). Phosphorylation of RyR2 at Ser^{1886} by these kinases was studied by means of sequence-specific antibodies that selectively recognize either the phosphorylated (phosphopeptide antibodies) or the nonphosphorylated serine residue (nonphosphopeptide antibodies). The phosphopeptide antibodies did not identify a phosphorylated serine residue (row 2), although sufficient amounts of substrate protein were available for all kinases (rows 3 and 4). Accordingly, nonphosphorylated Ser^{1886} was detected by nonphosphopeptide antibodies in this mutant RyR2 presented in different degrees of purity (row 1). Thus, the mutation-created Ser^{1886} is unlikely to be a target of any of the tested kinases.

SOICR in HEK293 cells expressing different RyR2 mutants

Single-cell Ca^{2+} imaging experiments with the stable, inducible HEK293 cell lines were carried out to assess their SOICR properties as described by Jiang et al. (8). These RyR2 expressing HEK293 cells are all sensitive to caffeine applied at the end of an experiment (Fig. 4, *left* and *right panels*). They also, with the notable exception of HEK cells expressing RyR2-G1885E/G1886S, readily developed SOICR activity when perfused with increasing $[Ca^{2+}]_o$. This leads to a time domain filled with Ca^{2+} transients before the final activation by 5 mM caffeine (Fig. 4, *middle panel*). In the experiment shown in Fig. 4, ~40–70% of the caffeine-sensitive HEK293 cells expressing RyR2-WT (41%), RyR2-G1885E (68%), RyR2-G1886S (49%), and RyR2-G1886D (59%), respectively, exhibited substantial SOICR (Fig. 4, *A–D*). In contrast, of a comparable number of 264 caffeine-responsive HEK293 cells expressing RyR2-G1885E/G1886S, only three (1%) showed significant Ca^{2+} release activity (Fig. 4 *E*). This markedly different SOICR behavior is summarized in Fig. 5 on the basis of four independent experiments. The number of cells showing SOICR compared with the total number of caffeine-responsive cells rises sigmoidally with increasing $[Ca^{2+}]_o$ for all RyR2 variants expressed (Fig. 5 *A*). So did the average number of Ca^{2+} transients per caffeine-responsive cell (Fig. 5 *B*) as well as the

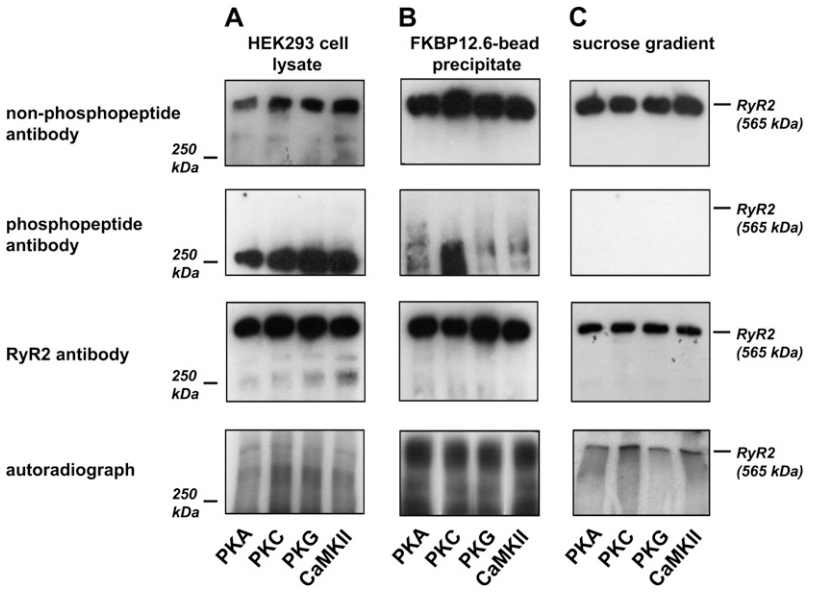

FIGURE 3 Phosphorylation of Ser^{1886} in RyR2-G1886S by various protein kinases. Three different types of RyR2-G1886S preparation were used as substrate for PKA, PKC, PKG, and CaMKII as indicated in the figure: (*A*) RyR2 in HEK293 cell lysate, (*B*) RyR2 immobilized to FKBP12.6-coupled beads, and (*C*) RyR2 enriched by sucrose density gradient centrifugation. After separation by SDS-PAGE, the proteins were immunoblotted with antibody against RyR2 (*row 3*), sequence-specific antibodies against a Ser^{1886}-containing peptide reflecting the potential RyR2 phosphorylation site (nonphosphopeptide antibody, *row 1*), and corresponding antibodies against a Ser1886(PO_3)-containing peptide (phosphopeptide antibody, *row 2*). Autoradiographs (*row 4*) demonstrate the phosphorylation of RyR2-G1886S by all of the protein kinases applied, but Ser^{1886} is no substrate of one of these tested kinases (compare *rows 1 and 2*).

average number of Ca^{2+} transients per Ca^{2+}-oscillating cell (Fig. 5 *C*). Because of the very low number of oscillatory active HEK293 cells expressing RyR2-G1885E/G1886S, reliable fits to the data could not easily be obtained in this case. Nevertheless, it is obvious that, on average, these cells are much less Ca^{2+} oscillating (Fig. 5, *A* and *B*) and, if so, show far fewer Ca^{2+} transients per active cell at a given $[Ca^{2+}]_o$ (Fig. 5 *C*) than the other RyR2-expressing cell lines. The data shown in Fig. 5 also suggest more subtle differences among these latter RyR2 variants, especially for RyR2-G1885E and -G1886D compared with RyR2-WT and -G1886S. A detailed analysis of the Ca^{2+}-oscillating behavior of individual cells of the different RyR2-expressing cell lines reveals essentially the same results (data not shown). The comparison of the $[Ca^{2+}]_o$-dependent SOICR activity of these cells isogenically expressing a defined RyR2 yields the following sequence of RyR2 channel activity:

$$\begin{aligned}\text{RyR2-G1886D} \approx \text{RyR2-G1885E} &> \text{RyR2-G1886S}\\ &> \text{RyR2-WT}\\ &\gg \text{RyR2-G1885E/G1886S}.\end{aligned}$$

In case of the double mutant RyR2-G1885E/G1886S, SOICR is nearly completely abolished.

Store Ca^{2+} load and Ca^{2+} transient amplitudes during SOICR activity

To determine whether the Ca^{2+} loading of the intracellular Ca^{2+} store is different or is changed differently during the single-cell Ca^{2+}-imaging experiments, the Ca^{2+} transients induced by 5 mM caffeine at the end of an experiment were compared among the different cell lines (Fig. 6 *A*). The amplitude of this transient, which reflects the Ca^{2+} loading of the store after a preceding history of SOICR, is similar for RyR2-WT, RyR2-G1886S, RyR2-G1886D, and RyR2-G1885E but strongly enhanced for RyR2-G1885E/G1886S (Fig. 6 *A*, *white bars*). This observation is in agreement with the $[Ca^{2+}]_o$-dependent SOICR activity described above, indicating that a substantial SOICR activity, as observed with HEK293 cells expressing the former RyR2 variants, is accompanied with a reduced steady-state Ca^{2+} loading of the internal store and a reduced threshold for SOICR. This interpretation is supported by the finding that caffeine-responsive HEK293 cells, which are not Ca^{2+}-oscillating during the perfusion with increasing $[Ca^{2+}]_o$, tend to respond to the caffeine challenge with enhanced Ca^{2+} transient amplitudes, reaching those of the barely Ca^{2+}-oscillating HEK293 cells expressing RyR2-G1885E/G1886S (Fig. 6 *A*, *gray bars*). The amplitudes of the SOICR events during the Ca^{2+} perfusion period were very similar for HEK293 cells expressing RyR2-WT, RyR2-G1886S, RyR2-G1886D, and RyR2-G1885E, respectively (Fig. 6 *B*). They reached ~70% of the final caffeine-induced Ca^{2+} transient amplitude independent of the actual $[Ca^{2+}]_o$. This indicates that for these RyR2-expressing cells, the individual SOICR event is a well-controlled process that always gives rise to a uniform Ca^{2+} transient. In case of the HEK293 cells expressing RyR2-G1885E/G1886S, the Ca^{2+} transient amplitude at 0.5 and 1 mM $[Ca^{2+}]_o$ reaches ~60% of the final caffeine-induced Ca^{2+} transient amplitude and drops to 30–40% at $[Ca^{2+}]_o <$ 0.5 mM. This indicates that here SOICR has not yet reached a consistent steady state during the $[Ca^{2+}]_o$ perfusion period and thus depends on the interplay between the actual state of Ca^{2+} store and that of the Ca^{2+} release channel, especially at lower $[Ca^{2+}]_o$.

DISCUSSION

The amino acid exchanges G1885E and G1886S investigated here, which are caused by ARVC-associated SNPs (13), are

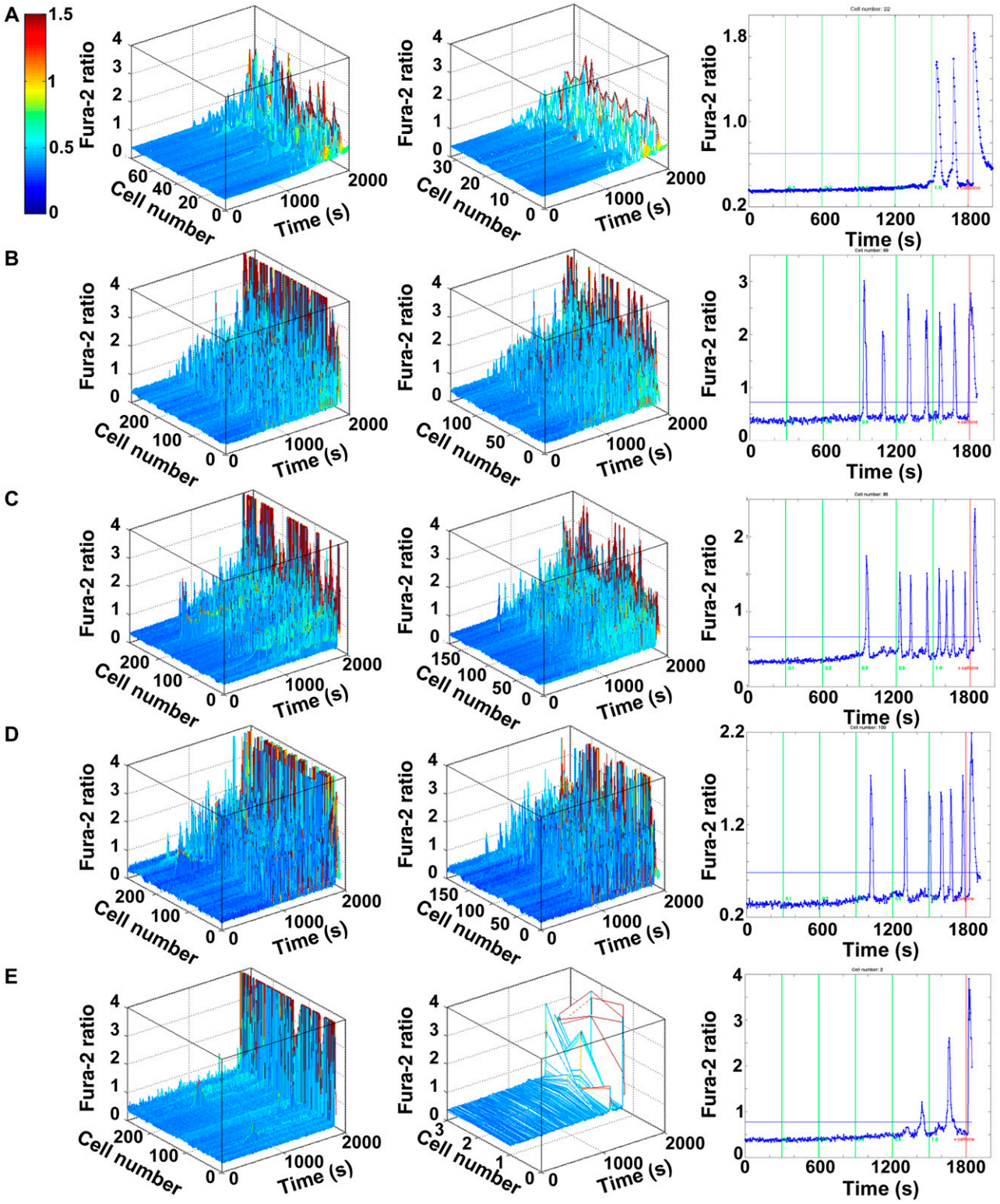

FIGURE 4 Single-cell fura-2 fluorescence recordings of HEK293 cells stably expressing RyR2-WT (*A*), RyR2-G1886S (*B*), RyR2-G1886D (*C*), RyR2-G1885E (*D*), and RyR2-G1885E/G1886S (*E*), respectively. The cells were successively incubated at increasing external Ca^{2+} concentrations, $[Ca^{2+}]_o = 0$, 0.1, 0.2, 0.3, 0.5, and 1.0 mM (5 min for each incubation period), followed by a final challenge with 5 mM caffeine in presence of 1.0 mM $[Ca^{2+}]_o$. (*Left panel*) Cells that are responsive to 5 mM caffeine added at the end of an experiment. Only these caffeine-responsive cells were subjected to further analysis of their Ca^{2+} oscillation behavior before this final challenge. They amount to 78, 281, 291, 286, and 264 cells (*A–E*) and may exhibit nontypical Ca^{2+} transients or no spontaneous Ca^{2+} transient at all before the caffeine treatment (see Experimental Procedures). (*Middle panel*) Truly Ca^{2+}-oscillating cells obtained after analyzing all individual traces shown in the left-hand panel. The numbers of cells remaining after this selection are 32, 137, 171, 195, and 3 cells (*A–E*). (*Right*

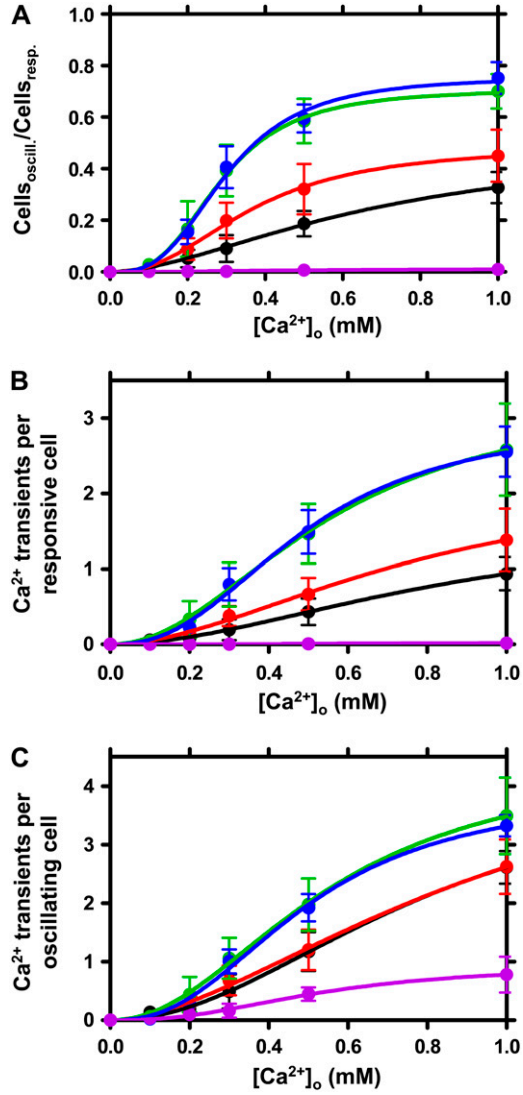

FIGURE 5 On average $[Ca^{2+}]_o$-dependent Ca^{2+}-oscillation behavior of HEK293 cells expressing a specific RyR2 variant. Shown are total mean ± SE of four independent experiments comprising several hundred cells for each RyR2-expressing cell line: RyR2-WT (*black*), RyR2-G1886S (*red*), RyR2-G1886D (*green*), RyR2-G1885E (*blue*), and RyR2-G1885E/G1886S (*magenta*). (*A*) Number of cells exhibiting spontaneous Ca^{2+} transients relative to the number of caffeine-responsive cells. (*B*) Average number of Ca^{2+} transients per caffeine-responsive cell. (*C*) Average number of Ca^{2+} transients per Ca^{2+}-oscillating cell.

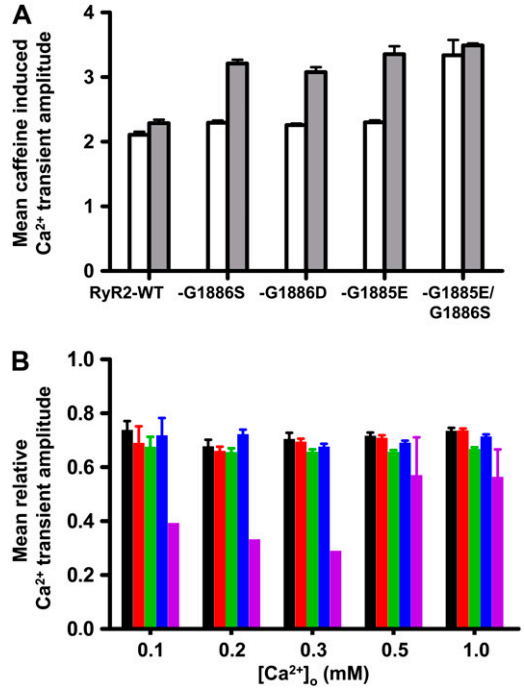

FIGURE 6 Amplitudes of caffeine-induced (*A*) and $[Ca^{2+}]_o$-dependent spontaneous Ca^{2+} transients (*B*) of HEK293 cells expressing different RyR2. Shown are Fura-2 ratios (total mean ± SE) of four independent experiments with RyR2-WT, RyR2-G1886S, RyR2-G1886D, RyR2-G1885E, and RyR2-G1885E/G1886S (colors in *B*: *black*, *red*, *green*, *blue*, and *magenta*, respectively). (*A*) Amplitudes of Ca^{2+} transients induced by 5 mM caffeine at the end of an experiment with HEK293 cells either showing (*white bars*; based on 200 to 690 cells for RyR2-WT, RyR2-G1885E, RyR2-G1886S, and RyR2-G1886D, and 19 cells for RyR2-G1885E/G1886S) or not showing (*gray bars*; several hundred cells in each case) spontaneous Ca^{2+} transients before the caffeine challenge. (*B*) Mean amplitudes of spontaneous Ca^{2+} transients observed in the $[Ca^{2+}]_o$ range indicated relative to the amplitude of the corresponding caffeine-induced Ca^{2+} transient obtained at the end of an experiment. The values for RyR2-G1885E/G1886S are based on nine oscillating cells, whereas those of all the other RyR2 variants were derived from a couple of hundred oscillating cells.

located in the divergent region 3 of RyR2 that is specific for cardiac muscle. This DR3 domain comprises residues 1852–1890 of RyR2 (6) and has been mapped to domain 9 in the clamp structure of RyR2 (20). The two glycine residues affected by the SNPs lay adjacent to the FKBP12.6 binding site, which recently has been assigned to the residues 1636–1937 (21). Because of the heterozygous combination of the two SNPs associated with ARVC in a subgroup of patients (13), carriers of this RyR2 genotype are not expressing wild-type RyR2 but RyR2 subunits that contain the amino acid exchange G1885E or G1886S in either a sole or combined fashion. In the study presented here, we have investigated homotetrameric RyR2 composed of subunits with either Glu^{1885} or Ser^{1886} in the DR3 domain, which reflect the former of the two possibilities mentioned before. A coex-

FIGURE 4 (Continued).
panel) Typical spontaneous Ca^{2+} transients of the cells shown in the middle panel. The horizontal lines indicate the individual thresholds used for definition of a SOICR event (see Experimental Procedures). The vertical green lines mark the 5-min time intervals that correspond to successively increasing $[Ca^{2+}]_o$. In the final interval marked by the red line, the cells were challenged with 5 mM caffeine in addition to 1 mM $[Ca^{2+}]_o$. The bar under *A* defines the color code used in the three-dimensional representations of the Fura-2 ratio levels.

pression of both RyR2 mutants in a single cell, which would reflect the second possibility, seems hardly possible considering the size of the gene, and even if successful, the actual subunit composition of the resulting functional RyR2 channel would not be known.

Expression of G1886S enabled us to study the phosphorylation of the putative PKC phosphorylation site introduced into RyR2 by one of the SNPs. The results show that RyR2-G1886S is a substrate of the protein kinases PKA, PKC, PKG, and CaMKII which are known to phosphorylate RyR2 (for review see Meissner (3)), but Ser^{1886} is not a target of any of these kinases used. This result refocuses attention from posttranslational modification back to the amino acid exchange itself at the position 1886 of RyR2. We have studied $[Ca^{2+}]_o$-dependent SOICR activity of HEK293 cells isogenically expressing the corresponding RyR2. Expression of RyR2-G1886S in comparison to RyR2-WT leads to a significant increase in the SOICR activity of the corresponding cells, which in turn indicates an enhanced RyR2 channel activity as a result of this mutation. The effect is even more pronounced for the mutation G1885E, which introduces an acidic residue into the DR3 domain in substitution of glycine. A similar enhanced SOICR activity was observed with HEK293 cells expressing RyR2-G1886D, initially included in the study to mimic a mutated RyR2 constitutively phosphorylated at Ser^{1886}. The effects of these two mutations, which both lead to replacement of glycine by an acidic amino acid at the positions 1885 and 1886, respectively, in the DR3 domain, are very similar. The DR3 region lies adjacent to the FKBP12.6 binding site of RyR2 and seems to be involved in the regulation of the Ca^{2+} release channel by physiological modulators such as ATP and Mg^{2+} (6). It is part of a cluster of domains of the RyR2 that undergo conformational change when the channel is switched from the closed to the open state (22,23). According to the results presented here, the glycine residues 1885 and 1886 represent a critical spot in the DR3 domain, which when replaced, especially by an acidic amino acid, lead to a destabilization of the channel reflected by increased SOICR activity at the cellular level and increased diastolic open probability at the single-channel level shown previously (13). It should be emphazised again, with respect to the composite heterozygous RyR2 genotype associated with ARVC (13), that carriers of this genotype could express singly mutated RyR2-G1885E and RyR2-G1886S in homotetrameric or heterotetrameric combinations. The homotetrameric RyR2 composed of either RyR2-G1885E or RyR2-G1886S studied here could be responsible for the enhanced lowest subconductance state of the Ca^{2+} release channel observed (13). But, according to the results presented here, tetramers composed of both singly mutated RyR2 types will presumably lead to a phenotype intermediate between a strongly destabilized RyR2-G1885E and a mildly destabilized RyR2-G1886S and thus to channel leakiness compared with wild-type RyR2.

It is very surprising that, when both mutations, G1885E and G1886S, each of which tends to induce enhanced channel activity, are combined in a single RyR2 subunit, RyR2-G1885E/G1886S, the channel activity is strongly inhibited. The characteristic blocking of the Ca^{2+} release channel in a closed state by 100 μM ryanodine was apparently preserved in this RyR2 mutant, but the Ca^{2+}-dependent ryanodine binding was significantly changed compared with the other RyR2 types studied. The sensitivity of RyR2-G1885E/G1886S to caffeine was significantly reduced, but the channel activation by 5 mM caffeine led to a typical substantial intracellular Ca^{2+} release in HEK293 cells expressing this doubly mutated RyR2. At the same time, the spontaneous SOICR activity of these cells was nearly completely blocked despite the fact that the Ca^{2+} loading of the intracellular store was rather increased. Thus, the combination in the same RyR2 subunit of the Ca^{2+} release-supporting amino acid exchange G1886S with the strongly Ca^{2+} release-promoting mutation G1885E surprisingly leads to a nearly complete shutdown of the spontaneous SOICR activity. It seems that the Ser^{1886} adjacent to Glu^{1885} stabilizes the Ca^{2+} release channel even above the level present in the wild-type RyR2. These results indicate that the residues 1885 and 1886 of RyR2 mark a sensitive spot inside the DR3 domain that is important for the control of the Ca^{2+} release properties of the channel. Because we were studying recombinant RyR2 expressed in HEK293 cells, the observed effects are caused solely by a direct modification of the channel protein itself. Whether the changes in the critical spot of the DR3 domain induced by the mutations might affect the FKBP12.6 binding site adjacent to the DR3 domain remains to be studied.

We greatly appreciate the gift of the PKA catalytic subunit from Dr. Friedrich Herberg, Universität Kassel, Germany.

This work was supported by the Deutsche Stiftung für Herzforschung grant F/22/05 to M. Varsányi.

REFERENCES

1. Fill, M., and J. A. Copello. 2002. Ryanodine receptor calcium release channels. *Physiol. Rev.* 82:893–922.
2. Bers, D. M. 2004. Macromolecular complexes regulating cardiac ryanodine receptor function. *J. Mol. Cell. Cardiol.* 37:417–429.
3. Meissner, G. 2004. Molecular regulation of cardiac ryanodine receptor ion channel. *Cell Calcium.* 35:621–628.
4. Yano, M., T. Yamamoto, Y. Ikeda, and M. Matsuzaki. 2006. Mechanisms of disease: ryanodine receptor defects in heart failure and fatal arrhythmia. *Nat. Clin. Pract. Cardiovasc. Med.* 3:43–52.
5. Liu, Z., J. Zhang, M. R. Sharma, P. Li, S. R. W. Chen, and T. Wagenknecht. 2001. Three-dimensional reconstruction of the recombinant type 3 ryanodine receptor and localization of its amino terminus. *Proc. Natl. Acad. Sci. USA.* 98:6104–6109.
6. Zhang, J., Z. Liu, H. Masumiya, R. Wang, D. Jiang, F. Li, T. Wagenknecht, and S. R. W. Chen. 2003. Three-dimensional localization of divergent region 3 of the ryanodine receptor to the clamp-shaped structures adjacent to the FKBP binding sites. *J. Biol. Chem.* 278:14211–14218.
7. Liu, Z., J. Zhang, R. Wang, S. R. W. Chen, and T. Wagenknecht. 2004. Location of divergent region 2 on the three-dimensional structure of

cardiac muscle ryanodine receptor/calcium release channel. *J. Mol. Biol.* 338:533–545.

8. Jiang, D., B. Xiao, D. Yang, R. Wang, P. Choi, L. Zhang, H. Cheng, and S. R. W. Chen. 2004. RyR2 mutations linked to ventricular tachycardia and sudden death reduce the threshold for store-overload-induced Ca^{2+} release (SOICR). *Proc. Natl. Acad. Sci. USA.* 101: 13062–13067.
9. Jiang, D., R. Wang, B. Xiao, H. Kong, D. J. Hunt, P. Choi, L. Zhang, and S. R. W. Chen. 2005. Enhanced store overload-induced Ca^{2+} release and channel sensitivity to luminal Ca^{2+} activation are common defects of RyR2 mutations linked to ventricular tachycardia and sudden death. *Circ. Res.* 97:1173–1181.
10. Oda, T., M. Yano, T. Yamamoto, T. Tokuhisa, S. Okuda, M. Doi, T. Ohkusa, Y. Ikeda, S. Kobayashi, N. Ikemoto, and M. Matsuzaki. 2005. Defective regulation of interdomain interactions within the ryanodine receptor plays a key role in the pathogenesis of heart failure. *Circulation.* 111:3400–3410.
11. Thomas, N. L., C. H. George, and F. A. Lai. 2006. Role of ryanodine receptor mutations in cardiac pathology: more questions than answers? *Biochem. Soc. Trans.* 34:913–918.
12. Paavola, J., M. Viitasalo, P. J. Laitinen-Forsblom, M. Pasternack, H. Swan, I. Tikkanen, L. Toivonen, K. Kontula, and M. Laine. 2007. Mutant ryanodine receptors in catecholaminergic polymorphic ventricular tachycardia generate delayed afterdepolarizations due to increased propensity to Ca^{2+} waves. *Eur. Heart J.* 28:1135–1142.
13. Milting, H., N. Lukas, B. Klauke, R. Körfer, A. Perrot, K. J. Osterziel, J. Vogt, S. Peters, R. Thieleczek, and M. Varsányi. 2006. Composite polymorphisms in the ryanodine receptor 2 gene associated with arrhythmogenic right ventricular cardiomyopathy. *Cardiovasc. Res.* 71:496–505.
14. Ho, S. N., H. D. Hunt, R. M. Horton, J. K. Pullen, and J. R. Pease. 1989. Site-directed mutagenesis by overlap extension using the polymerase chain reaction. *Gene.* 77:51–59.
15. Li, P., and S. R. W. Chen. 2001. Molecular basis of Ca^{2+} activation of the mouse cardiac Ca^{2+} release channel (ryanodine receptor). *J. Gen. Physiol.* 118:33–44.
16. Javois, L. C. 1999. Immunocytochemical Methods and Protocols, 2nd ed., Humana Press, Clifton, NJ. 11–18.
17. Kong, H., R. Wang, W. Chen, L. Zhang, K. Chen, Y. Shimoni, H. J. Duff, and S. R. W. Chen. 2007. Skeletal and cardiac ryanodine receptors exhibit different responses to Ca^{2+} overload and luminal Ca^{2+}. *Biophys. J.* 92:2757–2770.
18. Liu, Z., R. Wang, J. Zhang, S. R. W. Chen, and T. Wagenknecht. 2005. Localization of a disease-associated mutation site in the three-dimensional structure of the cardiac muscle ryanodine receptor. *J. Biol. Chem.* 280:37941–37947.
19. Xiao, B., G. Zhong, M. Obayashi, D. Yang, K. Chen, P. Walsh, Y. Shimon, H. Cheng, H. Ter Keurs, and S. R. W. Chen. 2006. Ser-2030, but not Ser-2808, is the major phosphorylation site in cardiac ryanodine receptors responding to protein kinase A activation upon beta-adrenergic stimulation in normal and failing hearts. *Biochem. J.* 396: 7–16.
20. Sharma, M. R., L. H. Jeyakumar, S. Fleischer, and T. Wagenknecht. 2006. Three-dimensional visualization of FKBP12.6 binding to an open conformation of cardiac ryanodine receptor. *Biophys. J.* 90:164–172.
21. Masumiya, H., R. Wang, J. Zhang, B. Xiao, and S. R. W. Chen. 2003. Localization of the 12.6-kDa FK506-binding protein (FKBP12.6) binding site to the NH2-terminal domain of the cardiac Ca^{2+} release channel (ryanodine receptor). *J. Biol. Chem.* 278:3786–3792.
22. Orlova, E. V., I. I. Serysheva, M. van Heel, S. L. Hamilton, and W. Chui. 1996. Two structural configurations of the skeletal muscle calcium release channel. *Nat. Struct. Biol.* 3:547–552.
23. Serysheva, I. I., M. Schatz, M. van Heel, W. Chui, and S. L. Hamilton. 1999. Structure of the skeletal muscle calcium release channel activated with Ca^{2+} and AMP-PCP. *Biophys. J.* 77:1936–1944.